ISSN 1330-3651 (Print), ISSN 1848-6339 (Online) https://doi.org/10.17559/TV-20221123025441
Preliminary communication

On Planning Algorithms for Free-Form Surface Machining Path under Fractal Theory

Wanjun LI

Abstract: The purpose of this research is to improve the machining efficiency of free-form surfaces. To this end, this paper analyses the calculation method of line spacing in the machining process of different tools, adopts the space-filling curve method in fractal theory under the premise of ensuring the machining scallop height to meet the accuracy requirements, and proposes a path generation algorithm based on the two-dimensional Hilbert curve in fractal theory. To solve the problems of tool path in the machining process such as machining efficiency and surface features, this paper innovatively sets the corresponding influence factors of the tool path, calculates the weights to determine the tool direction, and generates a tool path with small and continuous values of the integrated function of weights. Doing so it avoids the lifting of the tool at the island or groove position and improves the overall machining efficiency and surface quality. Compared with the related algorithms, the proposed algorithm improves the overall machining efficiency by 20% under the precondition of satisfying the machining quality. Examples also verify the feasibility and practicality of the tool path.

Keywords: free-form surfaces; fractal theory; path planning

1 INTRODUCTION

The tool path planning of complex parametric surfaces has been one of the key topics of computer numerical control (CNC) machining technology research. With growingly higher processing requirements of complex parametric curves and surfaces in aerospace, shipbuilding, automotive and other industrial manufacturing fields, the ability to process complex parametric curves and surfaces with high speed and high accuracy has become an important symbol of the processing capability of modern CNC systems. Experts at home and abroad have conducted a lot of research in this regard [1-7]. OuYang et al. [3] studied the algorithm of free-form three-axis CNC machining, and proposed a tool size adaptive selection algorithm based on Voronoi diagrams and Delaunay triangulation. Jensen et al. [4] proposed a curvature analysis method for adaptive selection of cutting tools by calculating surface curvature. Li and Zhang [5] proposed a tool planning method for five-axis CNC machining by surface discretization. Ding et al. [6] avoided interference-free surface machining by continuously dividing the surface for three-axis CNC machining and determining the cutting tool based on the maximum curvature point on the surface. Aiming to machine a better surface finish, Chiou and Lee [7] constructed a potential field to select the maximum machining bandwidth as the basis for selecting the tool path of the parallel structure. With the aim of reducing machining time for higher machining efficiency, Kim and Sarma [8] used a greedy algorithm to calculate the direction of the parallel structure toolpath with the shortest machining time. A study by Yang et al. [9] planned an equi parametric toroidal structure tool path method by projecting a three-dimensional free-form surface to be machined into the two-dimensional parametric plane. Based on the previous studies, Kim [10] modified and applied them to the toolpath planning of complex cavity-type machined parts containing hollow islands. Sun et al. [11] mapped the 2D planar spiral toolpath onto the 3D free-form surface to generate a spiral toolpath. Based on the study by Zhouet al. [12] they improved the design of a double spiral toolpath suitable for high-speed machining. The principle of a space-filling toolpath is to fill the entire free-form surface with a large number of linear segments, which in theory can fill the entire surface. Moodleah and Makhanov [13] were the first to use the space-filling method in the design of free-form components, effectively reducing the total length of the toolpath. Based on Makhanov's research, Lin et al. [14] creatively proposed to combine the space-filling structure with the tool contact mesh to streamline the U-shaped structure generated within the space-filling, which has improved the machining performance of the machine tool. Based on Lin's research direction, Ma et al. [15] proposed a tool positioning mesh, adding the cutting force constraint to the space-filling structure. The iso parametric line method [16-19] is the simplest method for toolpath planning. In free-form surfaces constructed using the non-uniform rational basis spline (NURBS) method, two parameters u and v are usually used to represent two different directions of the surface. The iso parametric line method is used to generate a toolpath covering the entire surface by keeping u or *v* constant and incrementing the other parameter at equal intervals. As this is an equal interval increment, the incremental interval is usually set at the line spacing of the point of greatest curvature change on the surface in order to meet the machining requirements for accuracy. When the curvature of the entire surface changes significantly, this results in redundant toolpaths and reduces machining efficiency. Hence, the iso parametric line method is mainly applied to surfaces with little surface change. The iso scallop height method [20-24] was started by Suresh et al. After refining by a large number of experts and scholars, the method has now developed into a more mature method of toolpath planning. Its core idea is to obtain the machining line spacing by making the scallop height between the corresponding tool contacts on the adjacent path equal to a fixed value. Compared with the iso parametric method, the iso scallop height method makes full use of the machining line spacing in the planning process with no tool redundancy. Hence, the machining efficiency is higher and the scallop height of the finished workpiece surface is uniform. The cross-section method [25-29] uses a set of parallel planes to intercept the machined surface, and the resulting intersection line is the toolpath line. One of the difficulties in toolpath planning with the cross-section method is the determination of the best attitude angle of the parallel planes relative to the

machined surface. To simplify the calculation, in general, when the curvature of the surface changes less, let the plane group be perpendicular to the machined surface. When the curvature of the surface changes a lot, let the plane group be parallel to the machined surface. The second difficulty is the intersection operation between the plane group and the machined surface.

There are three main types of path generation algorithms for machining complex parametric surfaces: the iso parametric line method, the constant section method, and the iso scallop height method. The iso parametric line method involves the tool moving in the *u* and *v* direction of the surface and is suitable for surfaces with a uniform distribution of parametric lines. Its advantage is that the toolpath calculation is small, but the disadvantage is that the toolpath is dense and long and the machining efficiency is not high. The tool follows the line of intersection between the surface and the equidistant section when machining using the constant section method. This method is suitable for surfaces with small curvature changes. Its advantage is that the toolpath calculation is small, but the disadvantage is that the section spacing is not easy to control, resulting in denser toolpaths on flat surfaces and sparser toolpaths on steeper surfaces, as well as low surface quality for machining. In contrast, the iso-scallop height method makes the scallop height of the path constant by controlling the distance between adjacent paths so that the next toolpath can be calculated on the premise that one machining path, the tool radius and the permissible scallop height are known. Clearly, this is an efficient machining method. Makhanov and Anotaipaiboon [30] have proposed to use space-filling curves as toolpaths, which have good continuity and uniformity of distribution over the parameter interval, essentially eliminating empty strokes throughout the machining process and reducing the total length of the toolpath line.

Based on the advantages and disadvantages as said above, this paper proposes a new path generation algorithm using the space-filling curve theory of the fractal principle while in line with the advantages of the iso-scallop height method to enable the generation of continuous and approximately shortest toolpaths.

2 EFFECTIVE CUTTING RADIUS AND CUTTING LINE SPACING CALCULATION

2.1 Effective Cutting Radius of the Tool

Five-axis CNC machine tools have two more degrees of freedom than three-axis ones, and the machining process can be adjusted by adjusting the tool attitude so that the tool is in an extremely favourable processing position on the processing surface, enabling it to achieve better processing quality and maximum cutting area. To improve the processing efficiency, you can use a flat bottom end mill cutter or circular milling cutter with good cutting effect and high efficiency for processing, so that the tool can achieve maximum cutting efficiency in the process.

When machining complex free-form surfaces with an end mill cutter, the theoretical position vector of the tool axis should be parallel to the surface normal vector ***n*** at the tool tip, while the flat bottom surface of the tool is in the tangential plane formed by the tangential vectors ***f***(***f*** is the direction of the cutting feed along the *CC* point) and ***b***(***b*** is determined by ***f*** and ***n*** according to the right-hand spiral rule). In practice, to avoid overcutting and tool touching during the machining of curved surfaces, the heel angle of the tool β and the side deflection angle α need to be adjusted. Fig. 1a to Fig 1c shows the three tool attitudes after adjusting the angle. By adjusting the tool attitude, the tool produces a tool attitude angle where the effective cutting surface of the flat bottom end mill cutter and the circular milling cutter is no longer the circular surface projected by the tool, but becomes a non-circular machining surface during the cutting process.

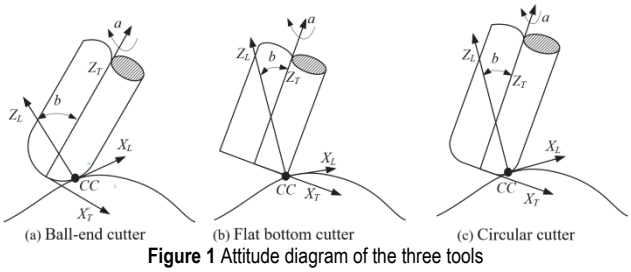

Figure 1 Attitude diagram of the three tools

As the tool attitude angle changes, the effective cutting radius of the tool is no longer a fixed value. Instead, it changes as the tool attitude changes. To accurately calculate the toolpath and to ensure that the cutting process does not produce repeated tool movements, the line spacing between the two paths needs to be accurately determined. In the actual calculation process, the line spacing is mainly calculated based on the effective cutting radius of the tool. The following analysis is carried out for circular, flat-bottom and ball-end tools respectively to derive the effective cutting radius of the tool.

(1) Calculation of the effective cutting radius of the flat-bottom cutter.

During the machining of a surface with a flat-bottom cutter, the tool attitude needs to be adjusted to avoid local and global interference by rotating the tool around the cutting point in the feed direction by an angle β, which is called the heel angle; the tool rotates around the normal vector of the cutting point by an angle α, which is called the side deflection angle, as shown in Fig. 2a.

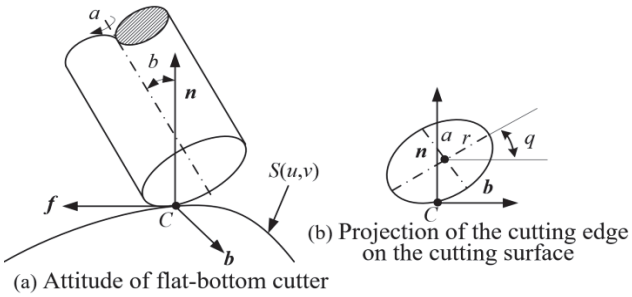

Figure 2 Effective cutting surface of flat-bottom cutter

After the tool is deflected, the actual effective cutting surface of the tool is no longer the circular surface at the end of the tool. The projection of the cutting edge in the tangent plane becomes an elliptical surface as shown in Fig. 2b. The effective cutting radius of the flat-bottom end mill cutter after deflection can be calculated by Eq. (1).

$$\begin{cases} a = r\sin\beta\cos\alpha \\ \theta = \tan^{-1}\left(\tan\beta\sin\alpha\right) \end{cases}$$

$$\frac{x^2}{a^2}+\frac{y^2}{r^2}=1 \tag{1}$$

$$R_e=\frac{1+\sin^2\beta\cos^2\alpha+(1+\sin\beta\cos\alpha)\sqrt{1+\sin^2\beta\cos^2\alpha}}{2\sin\beta\cos\alpha}\times R$$

where β, α - the positioning angle for the tool attitude in multi-axis machining, R - flat-end cutter radius, R_e - Effective cutting radius of the flat-end cutter during machining.

(2) Calculation of effective cutting radius of circular cutter.

During machining with a circular milling cutter, the principle is similar to that of a flat-bottom end mill cutter. To avoid interference during the cutting process, the heel angle β and the side deflection angle α values need to be determined. In practice, it is very difficult to calculate the side deflection angle. Hence, to simplify the calculation during the programming of CNC machining, priority is given to the adjustment of the heel angle β during the initial adjustment of the tool attitude. Set the side deflection angle of the tool α to zero. Then eliminate interference by adjusting the side deflection angle α if interference cannot be avoided by adjusting the heel angle β alone. The projection of the circular tool in different planes, as shown in Fig. 3 and Fig. 4, shows that different tool paths generate different effective cutting radii for the tool.

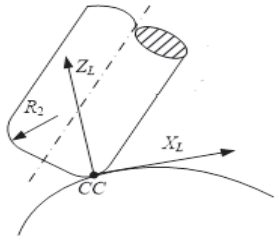

Figure 3 Radius of curvature in the $X_L - Z_L$ plane

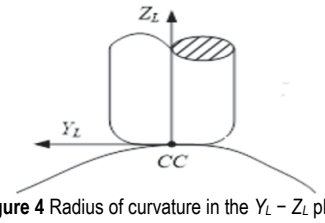

Figure 4 Radius of curvature in the $Y_L - Z_L$ plane

If the circular face of the circular cutter is machined parallel to the direction of travel, the effective radius of cut in that direction is given by Eq. (2).

$$R_{e\_XZ}=R_2=r \tag{2}$$

where r is the fillet radius of the circular cutter.

If the circular cutter is machined along the perpendicular to the direction of travel, the effective cutting radius can be found by Eq. (3).

$$R_{e\_YZ}=\frac{R+r\sin\alpha}{\sin\alpha} \tag{3}$$

(3) Calculation of the effective radius of the ball-end cutter.

The effective cutting radius is the radius of the tool itself due to the normal adaptive nature of the ball-end milling cutter in the machining process, as can be seen from Eq. (4).

$$R_e=R \tag{4}$$

2.2 Calculation of the Line Spacing of the Tool

The calculation accuracy of the cutting line spacing during toolpath planning has a direct bearing on the surface quality and efficiency. If the calculated line spacing between toolpaths is smaller than the actual line spacing to meet the scallop height, duplicate cuts will occur with longer machining time. If the calculated line spacing between toolpaths exceeds the actual cutting line spacing of the tool, the scallop height of the machined surface increases, reducing surface quality and requiring the tool to be moved again. This would make the overall machining of the surface less efficient. Therefore, accurate calculation of the cutting point distance is an important tool to ensure machining quality and improve machining efficiency.

When calculating the cutting distance, the geometrical parameters involved in the machining process are different for different types of tools. To simplify the calculation process, the following is a study of ball-end cutter as the object of the cutting line spacing calculation formula. With the effective cutting radius of the flat-bottom milling cutter and circular cutter instead of the radius of ball-end cutter, you can determine the corresponding line spacing calculation formula for different types of tools.

The following analysis is based on the study of ball-end milling cutter.

(1) Calculation of line spacing when machining flat surfaces.

When machining a flat surface with a ball end milling cutter, as shown in Fig. 5, the size of the cutting line spacing of the tool is closely related to the radius of the tool and the scallop height of the machining. With Eq. (5) and the transformation Eq. (6), we obtained the line spacing value L.

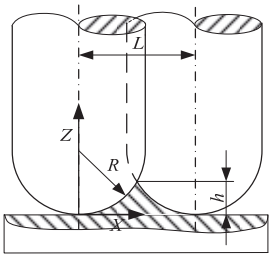

Figure 5 Line spacing for flatwork

$$(R-h)^2+\left(\frac{L}{2}\right)^2=R^2 \tag{5}$$

$$L=2\sqrt{R^2-(R-h)^2}=2\sqrt{2Rh-h^2} \tag{6}$$

In the actual machining process, the cutting tool radius $R >> h$, so the h^2 in Eq. (6) can be regarded as a tiny amount to be discarded, and Eq. (6) is simplified to obtain Eq. (7).

$$L = 2\sqrt{2Rh} \tag{7}$$

where L is the tool-to-tool line spacing and h is the scallop height.

Eq. (7) is the cutting line spacing of a ball-end cutter during the machining of a flat surface. To obtain the line spacing values for other types of tools during machining, simply replace the tool radius value R in the equation with the effective cutting radius R_e of a flat-bottom cutter, a circular cutter and a common milling cutter.

When calculating the line spacing using the simplified Eq. (7), the calculation result makes the line spacing value larger, which ultimately increases the scallop height value of the machining process. In order not to affect the surface quality, the scallop height value h needs to be reduced appropriately during the calculation process, which can be calculated by Eq. (6) and Eq. (7) to obtain the changed scallop height value as shown in Eq. (8). Subtracting the scallop height value by the actual scallop height value and then plugging it into Eq. (8), we obtained the corrected cutting line spacing.

$$\Delta h = \frac{h^2}{2R} \tag{8}$$

(2) Calculation of line spacing during concave surface machining:

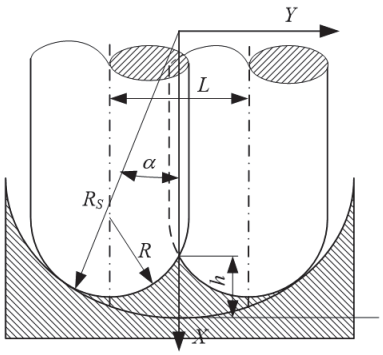

Figure 6 Spacing between concave machining lines

When the tool is machining a concave surface, the tool is machined in the attitude shown in Fig. 6. A suitable coordinate system is established and the distance is calculated as shown in Eq. (9).

$$(x-(R_s-R)\cos a)^2+(y-(R_s-R)\sin a)^2=R^2 \tag{9}$$

of which:

$$\cos\alpha=\sqrt{1-\left(\frac{L}{2(R_s-R)}\right)^2},\ \sin\alpha=\left(\frac{L}{2(R_s-R)}\right).$$

Substitute $x = R_s - h$, $y = 0$ into the above equation. Because $R_s >> h$, we obtained the following by simplified approximate.

$$L = 2\sqrt{2hR}\sqrt{\frac{R_s}{R_s-h}} \tag{10}$$

where R_s is the radius of curvature at the surface point. When using flat-bottom cutters, circular cutters and ordinary milling cutters for machining concave surfaces, it is very difficult to obtain an exact expression for the cutting line spacing. The effective cutting radius values calculated for different types of tools can be brought into Eq. (10) for calculation to obtain the corresponding line spacing.

For concave surfaces, the line spacing values obtained during the calculation of the line spacing are approximate and the scallop height values change, which can then be obtained from Eq. (11). If the Δh value exceeds the required accuracy value, the scallop height value between the two trajectories can be corrected by correcting the h value to ensure a constant scallop height value.

$$\Delta h = h\cdot\frac{2R_s^3h-12R_s^2Rh-4R_s^2h^2-8R(R_s+R)h^2+12R_sR^2h+R_sh^3}{8R(R_s+R)(R_s+h)^2} \tag{11}$$

(3) Calculation of line spacing during convex surface machining.

When machining convex surfaces, as shown in Fig. 7, the relationship is given in Eq. (12) based on the geometry in the figure, and the line spacing L *is* obtained by simplifying it as shown in Eq. (13).

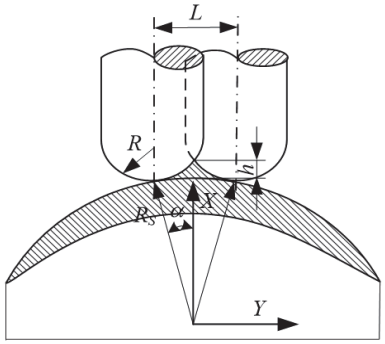

Figure 7 Spacing of convex surface machining rows

$$\left(x-(R_s+R)\cos\alpha\right)^2+\left(y-(R_s+R)\sin\alpha\right)^2=R^2 \tag{12}$$

where $\cos\alpha=\sqrt{1-\left(\frac{L}{2(R_s+R)}\right)^2}$ and $\sin\alpha=\left(\frac{L}{2(R_s+R)}\right)$.

$$L = 2\sqrt{2hR}\sqrt{\frac{R_s}{R_s+h}} \tag{13}$$

Similarly, it is very difficult to obtain an accurate expression when calculating the line spacing for convex surfaces using flat-bottom cutters, circular cutters and common milling cutters, so the effective cutting radius values of flat-bottom cutters and circular cutters calculated above can be substituted into Eq. (13) to simplify the calculation, thus obtaining the corresponding line spacing values for flat-bottom cutters and circular cutters.

When deriving the cutting line spacing for convex surfaces, the line spacing is varied due to the simplification of the data, and the corresponding change in scallop height value can be derived from Eq. (14). If the change in scallop

height value is out of tolerance, the scallop height h is corrected and then substituted into Eq. (13) to obtain the modified cutting line spacing value, ensuring a constant scallop height value between paths.

$$\Delta h = h \cdot \frac{4R_s^3 h + 12R_s^2 Rh + 4R_s^2 h^2 + 8R(R_s + R)h^2 + 12R_s R^2 h + R_s h^3}{8R(R_s + R)(R_s + h)^2} \quad (14)$$

In the process of CNC milling, the main cutting tools used are flat-bottom cutters, ball-end cutters and circular cutters. The common milling cutters are rarely used and are mainly used in three-axis milling machines. When calculating the cutting distance of common milling cutters, due to the complexity of their own structure, the process of calculating the distance of the line should be analysed in a variety of situations, which will not be detailed in this paper.

3 RESEARCH ON ADAPTIVE TOOLPATH PLANNING ALGORITHMS

3.1 Calculation of Parameters for the Iso-Scallop Height Method

Let the parametric equation of the surface to be machined be:

$$S(u, v) = \{x(u, v), y(u, v), z(u, v)\} \quad (15)$$

The scallop height h of the surface is a function of the distance L between the two cutting lines, the effective cutting radius R of the tool, and the normal radius of curvature R^* of the surface along the line spacing. Obviously, the greater the distance between two adjacent cutting lines, the greater the scallop height. Conversely, if the scallop height value is kept constant, the spacing between the two cutting lines should be determined by the normal curvature radius of the surface in the line spacing direction. There are in fact an infinite number of curves perpendicular to the known toolpath at a given point on the surface, and the adjacent toolpath should be the one with the shortest distance from the known toolpath line at that point. According to differential geometry theory, the incremental parameter values Δu and Δv corresponding to the scallop height paths using parametric surfaces are shown in Eq. (16).

$$\Delta u = \frac{\pm L\left(F\frac{\mathrm{d}u}{\mathrm{d}t} + G\frac{\mathrm{d}v}{\mathrm{d}t}\right)}{\sqrt{EG - F^2}\sqrt{E\left(\frac{\mathrm{d}u}{\mathrm{d}t}\right)^2 + 2F\frac{\mathrm{d}u}{\mathrm{d}t}\frac{\mathrm{d}v}{\mathrm{d}t} + G\left(\frac{\mathrm{d}v}{\mathrm{d}t}\right)^2}}, \quad \Delta v = \frac{\pm L\left(E\frac{\mathrm{d}u}{\mathrm{d}t} + F\frac{\mathrm{d}v}{\mathrm{d}t}\right)}{\sqrt{EG - F^2}\sqrt{E\left(\frac{\mathrm{d}u}{\mathrm{d}t}\right)^2 + 2F\frac{\mathrm{d}u}{\mathrm{d}t}\frac{\mathrm{d}v}{\mathrm{d}t} + G\left(\frac{\mathrm{d}v}{\mathrm{d}t}\right)^2}} \quad (16)$$

where Δu is the incremental value of the parametric surface u, Δv is the incremental value of the parametric surface v, E, F, G is the first fundamental in differential geometry, and L, M, N is the second fundamental.

The parameter value of the iso-scallop height path is obtained from Eq. (16) and another path line P_1 with a constant scallop height adjacent to the current tool path point $P(u(t), v(t))$ can be found by connecting the corresponding tool points, which is obtained from Eq. (17).

$$P_1 = P\left(u(t) + \Delta u(t), v(t) + \Delta v(t)\right) \quad (17)$$

3.2 Iso-Scallop Height Toolpath Generation

With Eq. (16), the iso-scallop height path parameters are calculated for the parametric surfaces u and the v direction respectively. In the process of calculating the parameter increments in the u or (v) direction, a starting point is determined for each machining path. To facilitate the calculation, an initial path line is established for the parameter u or (v), which can be taken as the initial path line with the boundary line of $u = 0$ or ($v = 0$). Also, a number of tool position points are taken from the path line as the calculation points for iso-scallop height. The parameter values u or (v) obtained during the calculation must satisfy Eq. (4) or Eq. (5). Substitute the obtained parameter values into Eq. (17) to obtain the toolpath with iso-scallop height values in the direction of u or (v).

$$0 \le u_{begin} \le u_i \le u_{end} \le 1 \quad (18)$$

$$0 \le v_{begin} \le v_i \le v_{end} \le 1 \quad (19)$$

u_{begin} is the initial boundary path parameter value in the u direction, u_{end} is the termination parameter value in the u direction; v_{begin} is the initial boundary path parameter value in the v direction, v_{end} is the termination parameter value in the v direction.

3.3 Combination of Iso-Scallop Height Method and Space-Filling Curve Method for Toolpath Generation

Adaptive space-fill curves as tool paths are characterised by: firstly, adaptive space-fill curves accompanied by an optimum direction; secondly, in contrast to conventional space-filling curves, adaptive space-filling curves only reverse when the optimum direction changes; thirdly, the adaptive space-filling curve eliminates maximum dynamic errors and corner-induced overcutting. Finally, locally encrypted adaptive space-fill curves are as accurate as conventional space-fill curves.

Considering the characteristics of the adaptive space-filling curve method, along with the advantages of the iso-scallop height method, we conducted toolpath planning for free-parametric surfaces.

Using the principle that the space-filling curve can fill every corner without any dead angle, adding an adaptive algorithm to ensure that the machining path follows the principle of maximum cutting rate and reduced auxiliary path, and combining the advantages of the method of equal residual height, the tool path planning is carried out on the free-parameter surface.

3.3.1 Intersection Finding and Loop Generation

The toolpaths with iso-scallop height values in the two parameter directions are calculated separately by Isoparametric method. The toolpaths in the two parameter directions are superimposed and the intersection point between the superimposed curves is found as the loop vertex.

(1) Intersection of curves.

Intersection of complex curves is a difficult problem and a hot topic of research. The most used free curve intersection algorithm is the envelope surface method. But this method is computationally intensive. Considering that the toolpaths of two covariates are in the same parameter plane, the spatial curves can be converted into two-dimensional parameter curves for intersection calculation. We used the Lagrange interpolation method to establish the parameter intersection of the curves, and then converted the parameter values obtained from Eq. (15) into three-dimensional coordinate values.

In the process of intersecting parametric curves, it is possible that a single parameter variable may represent multiple surface points in a spatial surface if, for example, there are vertical surfaces. In this case, the scallop height path is used to determine the true surface coordinate points by the columns or rows of the path, avoiding the problem of a single parameter representing multiple data points that cannot be distinguished. Once the parameter values for the intersection points are obtained, the surface equations are used to establish the coordinates of the intersection points of the spatial curves. This method has been proven to reduce the calculation time for curve intersections and to reduce the time required to assist in the CNC machining process.

(2) Loop generation.

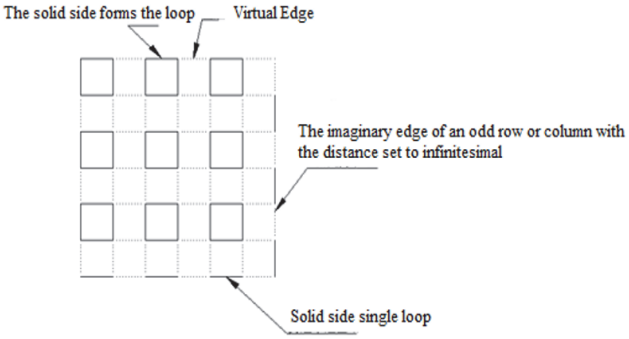

Figure 8 Loop division

A modified space-filling curve method combines all the intersections into small disconnected loops, which are combined into a single Hamiltonian loop, initially formed by constructing small rectangular loop paths. The vertices of the even rows and columns are connected to the vertices of the adjacent odd rows and columns through the vertices of the even rows and columns. Thus, if m and n are odd, any boundary point in *m* and *n* is first constructed as a single loop, i.e., two adjacent boundary points and the added real line form a closed loop, as shown in Fig. 8.

At this point, the surface circuit is considered to be an undirected graph in fractal science, with each adjacent point connected by an edge. The vertices in the graph are the surfaces where the corresponding initial tool contact points are located, and the distance between the two vertices is the distance between the two tool contacts in 3D space. Since all points are iso-scallop height path points on the surface and satisfy iso-scallop height values, the tool path can optimally pass through the space filling curve.

3.3.2 Path Planning

(1) Improved space-filling curve algorithm.

Loop *A* and its neighbouring loops *B*, *C*, *D* and *E* are first analysed to establish the value of the Total function, which is determined by a combination of tool attitude, machining conditions, shape of the machined surface and the spacing between neighbouring tool position points. The Total value is established by combining the surface shape and its tool position point spacing. The corresponding Total functions are compared and the circuit with the lowest value is selected as the direction for generating the toolpath.

$$\begin{aligned}&\mathrm{Min}\left[Total\left(A,B\right),Total\left(A,C\right),\right.\\&\left.,Total\left(A,D\right),Total\left(A,E\right)\right]\end{aligned}\tag{20}$$

A minimum value is obtained from Eq. (20), assuming that the combined influence function between loops *A* and *B* has the smallest value, as in Fig. 9a to Fig. 9b is a merging process, where two adjacent loops are able to merge into one large loop. The merging process is defined by Eq. (21) as

$$Merge\left(A,B\right)=|c|+|d|-|a|-|b|\tag{21}$$

where *a*, *b* are edges connected by two vertices in 3D space. *c*, *d* are imaginary edges of two adjacent points in 3D space.

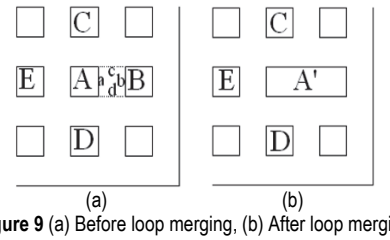

Figure 9 (a) Before loop merging, (b) After loop merging

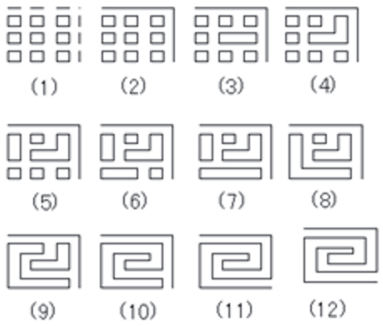

Figure 10 Tool path generation process

If the number of rows and columns at the intersection point is odd, then the Total value of the dashed edges between the remaining rows or columns after forming the smallest loop is first set to infinity, indicating that the

remaining edges are first joined into a single toolpath as the initial merge, and the rest of the mesh is formed into a Hamiltonian path by deleting the corresponding dashed edges. Merging all small loops produces a new loop, as in Fig. 9a where loops *A* and *B* are merged to form loop *A*' in Fig. 9b. Continue to calculate the value of the Total function by using Eq. (20), and in turn, once all loops have been merged, the required tool path is generated, Fig. 10 shows the path generation process.

(2) Algorithmic steps.

Let *T* be the set of edges with the smallest Total value, and merge as follows.

1) Let *T* = empty set and sort the vertices in increasing order of the calculated Total values. If there is a case of equal Total values, sort the vertices of the two solid loops first and consider the dashed vertices second.

2) Search for loops that are not visited, including the case of loops that have been merged inside *T* and do not form loops with other edges inside *T* or form independent loops with other edges in *T*. However, in the process of merging loops, a small lattice loop consisting of four edges is merged with a maximum of three edges, otherwise there will be independent loops that cannot be merged further in.

3) If this edge exists in *T*, sort it according to the size of Total, merge the two vertices corresponding to the two loops with the smallest Total, connect the two nearest vertices, add the corresponding edge and skip to step 4, otherwise skip to step 2.

4) If *T* includes $n - 1$ of these merges (*n* is the number of lattice loops formed), stop and output the Hamiltonian loops, otherwise go to step 2.

4 SIMULATION EXAMPLE VALIDATION

To verify the effectiveness of the algorithm, path planning was carried out for two complex free-form surface models with multiple islands. Under the same parameter conditions, the residual height is 0.01 mm, feed speed is 2000 mm/min, spindle speed is 6000 r/min, compare with the line tangent path generation algorithm in the UG software.

As shown in Fig. 11 and Fig. 12, the toolpath generated in UG has multiple lifted toolpaths around the island to exit the cutting phenomenon, while the algorithm proposed in this paper avoids the island well, with no lifted tool and continuous toolpath. The two algorithms were compared. As shown in Tab. 1, due to the optimization in the calculation time of toolpath, the algorithm proposed in this paper uses a longer time compared to the tool path algorithm in UG. But the algorithm proposed in this paper has no lifting phenomenon, while the toolpath generated in UG has 42 times and 120 times of lifting. The algorithm proposed in this paper generated all the path as the machining path, and the auxiliary path is zero. There are more auxiliary paths in the ones generated by UG. The overall length of the toolpaths generated by the algorithm proposed in this paper is shorter, and the tool is always in the machining state during the machining process, which is more stable than the paths generated by UG and improves the overall machining efficiency. The experiments show that all the trajectories generated by this algorithm are machining trajectories, and the auxiliary trajectories are zero. There are many auxiliary trajectories in UG. The overall length of the tool path generated by the proposed algorithm is short, and the tool path generated by the algorithm is more stable than that generated by UG, and the overall machining efficiency is increased by 20%.

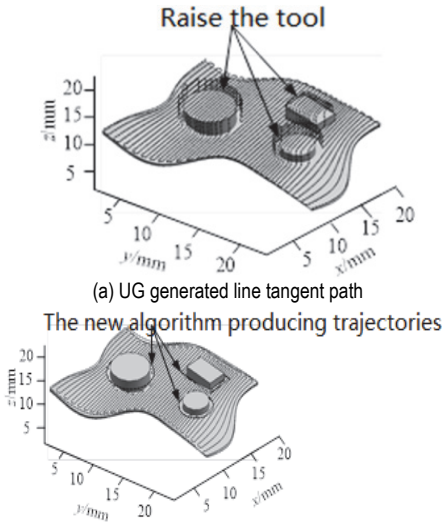

(a) UG generated line tangent path

(b) Toolpath for the algorithm in this paper

Figure 11 Path generation for complex surface with island type

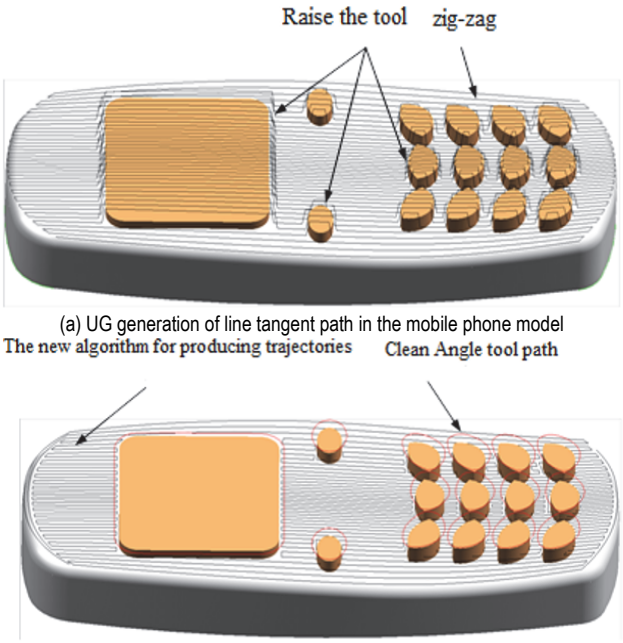

(a) UG generation of line tangent path in the mobile phone model

(b) Path under this paper's algorithm in the mobile phone model

Figure 12 Path generation for the mobile phone model

Table 1 Comparison of the two algorithms

Algorithm name	Lifting / times	Toolpaths / quantity	Calculation time / s	Total length of path / mm
Algorithm in UG (Fig. 5)	42	43	29.29	519.630
Algorithm in this paper (Fig. 5)	0	1	47.68	365.487
Algorithm in UG (Fig. 6)	120	121	117.72	5455.449
Algorithm in this paper (Fig. 6)	0	1	166.02	3339.773

5 CONCLUSION

The improved Hilbert curve was used to plan the path of a complex surface with multiple islands, generating a continuous toolpath that traverses the entire surface without lifting the tool, while meeting the accuracy requirements. In comparison with the path algorithm in UG, the tool path length is short, the whole tool path is shortened by 30%, there is no cut-in in the machining process, and the machining is stable. For complex multi-island surfaces, the tool paths generated by the algorithm are all cutting paths. The tool path generated inherits the advantages of the equal residual height method and the space-filling curve method, meets the machining accuracy requirements, and can completely cover the entire surface.The simulation demonstrates that this method can generate the shortest and continuous toolpaths, avoid multiple tool lifts during machining, and shorten the toolpath length while improving machining efficiency.

6 REFERENCES

[1] Giordano, A., Diourté, A., Bordreuil, C., Bugarin, F., & Segonds, S. (2022). Thermal scalar field for continuous three-dimensional toolpath strategy using wire arc additive manufacturing for free-form thin parts. computer-aided design. *Computer-Aided Design*, *151*. https://doi.org/10.1016/j.cad.2022.103337

[2] Xiao, N., Liu, Y. Y., Zhang, X. Y., & Liu, Y. (2020). Swing angle error compensation of a computer numerical control machining center for special-shaped rocks. *Journal Européen des Systèmes Automatisés*, *53*(3), 369-375. https://doi.org/10.18280/jesa.530307

[3] Ou Yang, D., Van Nest, B. A., & Feng, H. Y. (2005). Determining gouge-free ball-end mills for 3D surface machining from point cloud data. *Robotics and Computer-Integrated Manufacturing*, *21*(4-5), 338-345. https://doi.org/10.1016/j.rcim.2004.10.003

[4] Jensen, C. G., Red, W. E., & Pi, J. (2002). Tool selection for five-axis curvature matched machining. *Computer-Aided Design*, *34*(3), 251-266. https://doi.org/10.1016/S0010-4485(01)00086-0

[5] Li, L. L. & Zhang, Y. F. (2006). An integrated approach towards process planning for 5-axis milling of sculptured surfaces based on cutter accessibility map. *Computer-Aided Design and Applications*, *3*(1-4), 249-258. https://doi.org/10.1080/16864360.2006.10738462

[6] Ding, X. M., Fuh, J. Y., & Lee, K. S. (2001). Interference detection for 3-axis mold machining. *Computer-Aided Design*, *33*(8), 561-569. https://doi.org/10.1016/S0010-4485(00)00097-X

[7] Chiou, C. J. & Lee, Y. S. (2002). A machining potential field approach to tool path generation for multi-axis sculptured surface machining. *Computer-Aided Design*, *34*(5), 357-371. https://doi.org/10.1016/S0010-4485(01)00102-6

[8] Kim, T. & Sarma, S. E. (2002). Toolpath generation along directions of maximum kinematic performance; a first cut at machine-optimal paths. *Computer-Aided Design*, *34*(6), 453-468. https://doi.org/10.1016/S0010-4485(01)00116-6

[9] Yang, D. C., Chuang, J. J., Han, Z., & Ding, S. (2003). Boundary-conformed toolpath generation for trimmed free-form surfaces via Coons reparametrization. *Journal of Materials Processing Technology*, *138*(1-3), 138-144. https://doi.org/10.1016/S0924-0136(03)00062-1

[10] Kim, H. C. (2010). Tool path generation for contour parallel milling with incomplete mesh model. *The International Journal of Advanced Manufacturing Technology*, *48*(5), 443-454. https://doi.org/10.1007/s00170-008-1733-9

[11] Sun, Y., Ren, F., Zhu, X., & Guo, D. (2012). Contour-parallel offset machining for trimmed surfaces based on conformal mapping with free boundary. *The International Journal of Advanced Manufacturing Technology*, *60*(1), 261-271. https://doi.org/10.1007/s00170-011-3577-y

[12] Zhou, B., Zhao, J., & Li, L. (2015). CNC double spiral tool-path generation based on parametric surface mapping. *Computer-Aided Design*, *67*, 87-106. https://doi.org/10.1016/j.cad.2015.06.005

[13] Moodleah, S. & Makhanov, S. S. (2015). 5-axis machining using a curvilinear tool path aligned with the direction of the maximum removal rate. *The International Journal of Advanced Manufacturing Technology*, *80*(1), 65-90. https://doi.org/10.1007/s00170-015-6958-9

[14] Lin, Z., Deng, X., Fu, J., & Gao, Q. (2018). An optimisation algorithm for reducing the number of turns on space-filling curve toolpath for sculptured surface milling. *International Journal of Computer Integrated Manufacturing*, *31*(2), 199-209. https://doi.org/10.1080/0951192X.2017.1407453

[15] Ma, J. W., Song, D. N., Jia, Z. Y., Hu, G. Q., Su, W. W., & Si, L. K. (2018). Tool-path planning with constraint of cutting force fluctuation for curved surface machining. *Precision Engineering*, *51*, 614-624. https://doi.org/10.1016/j.precisioneng.2017.11.002

[16] He, W., Lei, M., & Bin, H. (2009). Iso-parametric CNC tool path optimization based on adaptive grid generation. *The International Journal of Advanced Manufacturing Technology*, *41*(5), 538-548. https://doi.org/10.1007/s00170-008-1500-y

[17] Lin, Y. J. & Lee, T. S. (1999). An adaptive tool path generation algorithm for precision surface machining. *Computer-Aided Design*, *31*(4), 237-247. https://doi.org/10.1016/S0010-4485(99)00024-X

[18] Broomhead, P. & Edkins, M. (1986). Generating NC data at the machine tool for the manufacture of free-form surfaces. *International Journal of Production Research*, *24*(1), 1-14. https://doi.org/10.1080/00207548608919706

[19] Loney, G. C. & Ozsoy, T. M. (1987). NC machining of free form surfaces. *Computer-Aided Design*, *19*(2), 85-90. https://doi.org/10.1016/S0010-4485(87)80050-7

[20] Suresh, K. &Yang, D. C. H. (1994). Constant scallop-height machining of free-form surfaces. *Journal of Engineering for Industry*, *116*(2), 253-259. https://doi.org/10.1115/1.2901938

[21] Held, M. & Spielberger, C. (2009). A smooth spiral tool path for high speed machining of 2D pockets. *Computer-Aided Design*, *41*(7), 539-550. https://doi.org/10.1016/j.cad.2009.04.002

[22] Tournier, C. & Duc, E. (2005). Iso-scallop tool path generation in 5-axis milling. *The International Journal of Advanced Manufacturing Technology*, *25*(9), 867-875. https://doi.org/10.1007/s00170-003-2054-7

[23] Li, H. & Feng, H. Y. (2002). Constant scallop-height tool path generation for three axis sculpture surface machining. *Computer-Aided Design*, *34*, 647-654. https://doi.org/10.1016/S0010-4485(01)00136-1

[24] Lee, Y. S. (1998). Non-isoparametric tool path planning by machining strip evaluation for 5-axis sculptured surface machining. *Computer-Aided Design*, *30*(7), 559-570. https://doi.org/10.1016/S0010-4485(98)00822-7

[25] Huang, Y. & Oliver, J. H. (1994). Non-constant parameter NC tool path generation on sculptured surfaces. *The International Journal of Advanced Manufacturing Technology*, *9*(5), 281-290. https://doi.org/10.1007/BF01781282

[26] Kiswanto, G., Lauwers, B., & Kruth, J. P. (2007). Gouging elimination through tool lifting in tool path generation for five-axis milling based on faceted models. *The International Journal of Advanced Manufacturing Technology*, *32*(3), 293-309. https://doi.org/10.1007/s00170-005-0338-9

[27] Chen, Z. C. & Song, D. (2006). A practical approach to generating accurate iso-cusped tool paths for three-axis CNC milling of sculptured surface parts. *Journal of Manufacturing Processes*, *8*(1), 29-38. https://doi.org/10.1016/S1526-6125(06)70099-8
[28] Bobrow, J. E. (1985). NC machine tool path generation from CSG part representations. *Computer-Aided Design*, *17*(2), 69-76. https://doi.org/10.1016/0010-4485(85)90248-9
[29] Suh, Y. S. & Lee, K. (1990). NC milling tool path generation for arbitrary pockets defined by sculptured surfaces. *Computer-Aided Design*, *22*(5), 273-284. https://doi.org/10.1016/0010-4485(90)90092-Q
[30] Makhanov, S. S. & Anotaipaiboon, W. (2007). *Advanced numerical methods to optimize cutting operations of five axis milling machines*. Springer Science & Business Media.

Contact information:

Wanjun LI
School of Intelligent Manufacturing,
Zibo Vocational Institute,
Zibo 255314, China
E-mail: 10796@zbvc.edu.cn